Mathematical Modelling and Applications
2026, Vol. 11, No. 2, pp. 28–40
https://doi.org/10.11648/j.mma.20261102.11

Research Article

Mathematical Modeling of the Impact of Temperature and Elevated Sickle Cell Concentration on MHD Blood Flow Through a Porous Atherosclerotic Channel

Kubugha Wilcox Bunonyo[1, *], Anasuodei Bemoifie Moko[2], Tamuno Boma Odinga-Israel[3]

[1]Department of Mathematics and Statistics, Federal University Otuoke, Yenagoa, Nigeria

[2]Department of Computer Science and Informatics, Federal University Otuoke, Yenagoa, Nigeria

[3]Department of Biochemistry, Rivers State University, Port Harcourt, Nigeria

Abstract

This study offers a comprehensive mathematical and computational investigation of the combined effects of temperature gradient and high sickle cell concentration on blood circulation through a porous atherosclerotic channel in the presence of an applied magnetic field. The model incorporates key physiological and physical mechanisms, including magnetohydrodynamics (MHD), heat transfer, mass transport, porous medium resistance, and chemical reaction effects, to simulate realistic blood flow behavior under pathological conditions. The governing equations for momentum, energy, and concentration were formulated using appropriate assumptions for incompressible, electrically conducting blood flow. These equations were non-dimensionalised to identify important controlling parameters such as the Hartmann number (magnetic field strength), Grashof number (thermal buoyancy), solutal Grashof number (concentration buoyancy), Prandtl number, Schmidt number, porosity parameter, and chemical reaction parameter. Analytical methods were employed to obtain solutions, which were further analyzed through graphical and computational techniques. The results reveal that increased sickle cell concentration significantly increases flow resistance, leading to a reduction in velocity and impaired blood circulation, particularly in the presence of arterial narrowing due to atherosclerosis. The temperature gradient plays a dual role: it enhances fluid motion through buoyancy effects while also influencing viscosity and thermal diffusion. The applied magnetic field introduces a Lorentz force that suppresses fluid velocity, thereby providing a potential mechanism for controlling abnormal blood flow. The study demonstrates that the interaction between magnetic field, temperature gradient, and sickle cell concentration has a significant impact on blood flow characteristics in porous, diseased arteries. This work contributes to the advancement of biomedical fluid dynamics by offering a more realistic model for analyzing blood flow in pathological environments. It has potential applications in the design of medical treatments, such as magnetic field-assisted therapy, targeted drug delivery, and improved diagnostic understanding of circulatory disorders associated with sickle cell disease and atherosclerosis.

Keywords

Mathematical Modelling, MHD Blood Flow, Sickle Cell Concentration, Temperature Effect, Porous, Atherosclerotic Channel

*Correspondence: Kubugha Wilcox Bunonyo (wilcoxbk@fuotuoke.edu.ng)

Received: 12 March 2026; **Accepted:** 23 March 2026; **Published:** 10 April 2026

1. Introduction

Blood is a specialized fluid tissue in the human body that plays a pivotal role in sustaining life. It performs critical functions including oxygen transport, immune defense, hormone distribution, and waste removal. The composition of blood includes plasma, red blood cells (RBCs), white blood cells (WBCs), and platelets. Blood is an electrolytic fluid composed of ions, proteins, and cells, allowing it to conduct electrical signals. The presence of red blood cells (RBCs) in the blood volume such as sickle and normal cells affects the dielectric properties and conductivity of blood. These factors are crucial in bio-impedance studies and biosensor applications. Red blood cells, RBCs exhibit deformability and consistent shape, contributing to uniform conductivity, and sickle RBCs are rigid and irregular, leading to alteration of flow channel, dynamics and electrical impedance. Atherosclerosis is a pattern of arteriosclerosis, a condition marked by the formation of anomalies in the artery walls known as lesions. This is a long-term inflammatory condition that affects a variety of cell types and is caused by high blood cholesterol. Because of the accumulation of atheromatous plaques, these lesions may cause the artery walls to narrow. Usually, there are no symptoms at first, but if they do appear, they usually start around middle life. Depending on the bodily portion or parts where the afflicted arteries are located, severe cases may lead to peripheral artery disease, coronary artery disease, stroke, or renal problems, Bunonyo and Amos [7]. Daniel *et al*. [17] conducted a study on anatomy, blood flow. In this study a mathematical model was formulated to investigate the flow of blood on the human vessels and organs through which blood flow in the body. Blood consists of two main components, namely, plasma (55%), the liquid portion of blood that contains water, electrolytes, proteins (such as albumin and fibrinogen), glucose, lipids, hormones, and waste products like urea. It serves as a medium for transporting cells and substances throughout the body. Bunonyo and Dagana [12] conducted a study to investigate the impact of mass concentration on viscoelastic fluid flow through a Non-porous channel. Abdelsalam and Vafai [1] theoretically examined pulsatile blood flow in a narrow artery driven by peristaltic waves, incorporating suspended particles and unsteady effects via the Womersley number. Abdullah et al. [2] explored magnetohydrodynamic (MHD) influences on blood flow through irregular stenoses, modeling blood as a micropolar fluid to capture rheological behavior. Employing finite difference methods for the unsteady nonlinear system, they quantified reductions in axial velocity, flow rate, and wall shear stress under transverse magnetic fields, underscoring MHD's potential for flow regulation in stenotic conditions. Acosta et al. [3] developed an efficient, unconditionally stable numerical method of characteristics for solving one-dimensional hyperbolic blood flow models in arterial networks. Compared to discontinuous Galerkin approaches, their algorithm reduces computational cost while handling high wave speeds, enabling applications in real-time simulations, multi-cycle analyses, and uncertainty quantification for clinical decision-making. Ahmed et al. [4] analysed transverse magnetic field effects on blood flow in arteries, treating blood as a Newtonian fluid under pulsatile conditions. Numerical solutions demonstrated magnetic induction reducing velocity profiles and wall shear stress, with implications for targeted drug delivery and flow modulation in magnetic environments. Alasakani et al. [5] identified key hemodynamic parameters affecting blood flow in human arteries via sensitivity analysis. Their computational approach prioritized stenosis severity, vessel compliance, and pulsatility, linking high wall shear stress gradients to atherogenesis sites. Amos and Ogulu [6] examined magnetic effects on pulsatile flow in constricted axisymmetric tubes, modelling blood as an electrically conducting fluid. Analytical solutions using Bessel functions showed Hartmann number damping velocity. Carotid intima-media thickness (IMT) and plaque were distinguished by Baroncini *et al.* [8] as separate reactions to cardiovascular risks, with plaques signifying localized lipid accumulation and IMT suggesting diffuse hypertrophy. Customized imaging for risk assessment was recommended by their cohort research. Therefore, it has been demonstrated that lipid-lowering techniques like statin therapy and lifestyle modifications positively affect RBC lipid composition, which may contribute to these strategies' atheroprotective benefits, Tziakas*et al*. [18]. The development of aberrant haemoglobin (HbS), which causes red blood cells to take on a sickle or crescent shape, is the hallmark of sickle cell disease (SCD), a genetic blood illness. These deformed cells have an impact on oxygen supply and blood flow, which can lead to a number of issues. In order to comprehend the electrical signals produced by cellular activity, recent biomedical research has investigated the electrochemical and piezoelectric characteristics of biological systems Bunonyo *et al*. [16]. An extremely high rate of childhood mortality (50 to 90%) has also been linked to sickle cell disease (SCD), Serjeant [19] and Bunonyo *et al*. [16]. One of the most prevalent genetic causes of disease and mortality worldwide is sickle cell anemia, the first genetic condition to be explained in terms of a gene mutation, Makani *et al*. [20]. A mutation in the haemoglobin gene (HbS) causes sickle cells, which are red blood cells with an aberrant crescent or sickle shape. These cells can cause discomfort and tissue injury because they are less flexible and can obstruct blood flow in tiny vessels, Rees et al. [21]. The concentration of sickle cells is the percentage or quantity of sickle red blood cells in a specific volume of blood sometimes causes stroke cohort of patients with homozygous sickle cell disease [9]. It is employed to evaluate sickle cell disease severity or progression. In this study, however, we will develop a mathematical model that illustrates how sickle cell mass concentration affects heat transport via the blood artery.

2. Mathematical Formulation

We will take into consideration a few fundamental presumptions in order to examine the impact of sickle cell concentration on blood flow through blood channels in the presence of a magnetic field.

2.1. Assumptions

The following presumptions should be taken into consideration when creating a system of mathematical models to examine the aforementioned issue:

1) Blood is incompressible and electrically conducting fluid
2) The flow is laminar and fully developed
3) The artery contains atherosclerotic narrowing or stenosed
4) The porous medium obeys Darcy's law
5) Sickle cell disease (SCD) changes red blood cells into rigid sickle shapes, increasing viscosity depends on sickle cellconcentration
6) External magnetic field B_0 is applied
7) There is an influence of solutal concentration gradient and heat source
8) The solutal concentration can be reduced with treatment on the rate of reaction

Following Bunonyo *et al*. [14], Bunonyo *et al*. [15], and the above assumptions, we present the flow models as:

2.2. MHD Momentum Equation

$$\rho_b \frac{\partial w^*}{\partial t^*} = -\frac{\partial P^*}{\partial x^*} + \mu_b \nabla^2 w^* - \sigma_e B_0^2 w^* - \frac{\mu_b \varphi}{k^*} w^* + \rho_b g \beta_T \left(T - T_\infty\right) + \rho_b g \beta_C \left(C - C_\infty\right) \tag{1}$$

2.3. Energy Equation

$$\rho_b c_{bp} \frac{\partial T^*}{\partial t^*} = k_{bT} \frac{\partial^2 T^*}{\partial y^{*2}} + Q_0 \left(T^* - T_\infty\right) + Q_1 \left(C^* - C_\infty\right) \tag{2}$$

2.4. Sickle Cell Concentration Equation with Treatment

$$\frac{\partial C^*}{\partial t^*} = D_m \frac{\partial^2 C^*}{\partial y^{*2}} - k_0 k_T \left(C^* - C_\infty\right) \tag{3}$$

The corresponding boundary conditions for equations (1)-(3) are:

$$\left.\begin{array}{l} w^* \neq 0, T^* = 0, C^* = 0 \quad \text{at } y^* = 0 \\ w^* = 0, T^* = T_w, C^* = C_w \text{ at } y^* = R_0 \end{array}\right\} \tag{4}$$

Following Amos and Ogulu [6], the sickle cell induced atherosclerosis in the channel is modeled as:

$$y^* = \begin{cases} R_0 & \text{at } 0 \le x^* \le d_0 \\ R_1 + \delta_1^* e^{a_1 t} \cos\left(\dfrac{2\pi x^*}{\lambda_1}\right) & \text{at } d_0 \le x^* \le \lambda_1 \\ R_2 + \delta_2^* e^{a_2 t} \cos\left(\dfrac{2\pi x^*}{\lambda_2}\right) & \text{at } \lambda_1 \le x^* \le d_2 \\ R_1 + R_2 + \delta_1^* e^{a_1 t} \cos\left(\dfrac{2\pi x^*}{\lambda_1}\right) + \delta_2^* e^{a_2 t} \cos\left(\dfrac{2\pi x^*}{\lambda_2}\right) & \text{at } d_2 \le x^* \le \lambda_2 \end{cases} \tag{5}$$

2.5. Dimensional Quantities

In order to make the models governing the flow through the blood channel dimensionless, we considered the dimensionless quantities as stated below:

$$\left.\begin{aligned}
&\theta=\frac{T^*-T_\infty}{T_w-T_\infty},\phi=\frac{C^*-C_\infty}{C_w-C_\infty},Gr=\frac{g\beta_T\left(T_w-T_\infty\right)R_0^3}{\upsilon^2},Gc=\frac{g\beta_C\left(C_w-C_\infty\right)R_0^3}{\upsilon^2},Rd_3=\frac{k_0k_TR_0^2}{\upsilon},\\
&Rd_2=\frac{Q_1\left(C^*-C_\infty\right)R_0^2}{k_{bT}\left(T_w-T_\infty\right)},M=B_0R_0\sqrt{\frac{\sigma_e}{\mu_b}},x=\frac{x^*}{\lambda},y=\frac{y^*}{R_0},w=\frac{w^*R_0}{\upsilon},t=\frac{\upsilon t^*}{R_0^2},\delta_1^*=\delta_1R_0,\\
&\delta_2^*=\delta_2R_0,\frac{1}{k}=\frac{\varphi R_0^2}{k^*},Pr=\frac{\mu_bc_b}{k_{Tb}},Rd_1=\frac{Q_0R_0^2}{\mu_bc_b},Sc=\frac{\upsilon}{D_m},h_1=\frac{R_1}{R_0},h_2=\frac{R_2}{R_0},x=\frac{x^*}{\lambda_1},x=\frac{x^*}{\lambda_2}
\end{aligned}\right\} \tag{6}$$

Using equation (6) on the governing equations (1)-(5), the governing equations are reduced to the following dimensionless equations governing the flow, which are:

$$\frac{\partial w}{\partial t}=-\frac{\partial P}{\partial x}+\frac{\partial^2 w}{\partial y^2}-M^2w-\frac{1}{k}w+Gr\theta+Gc\phi \tag{7}$$

$$Pr\frac{\partial\theta}{\partial t}=\frac{\partial^2\theta}{\partial y^2}+\theta PrRd_1+\phi Rd_2 \tag{8}$$

$$\frac{\partial\phi}{\partial t}=\frac{1}{Sc}\frac{\partial^2\phi}{\partial y^2}-Rd_3\phi \tag{9}$$

Using the conditions in equation (6) in simplifying equation (5), the sickle cell induced atherosclerosis in the channel is transformed into:

$$y=\begin{cases}1 & \text{at } 0\le x\le\dfrac{d_0}{\lambda}\\ h_\alpha=h_1+\delta_1e^{a_1t}\cos\left(2\pi x_1\right) & \text{at } \dfrac{d_0}{\lambda_1}\le x\le 1\\ h_\beta=h_2+\delta_2e^{a_2t}\cos\left(2\pi x_2\right) & \text{at } 1\le x\le\dfrac{d_2}{\lambda_2}\\ h_\gamma=\left(h_1+h_2\right)+\left(\delta_1e^{a_1t}+\delta_2e^{a_2t}\right)\cos\left(2\pi x\right) & \text{at } \dfrac{d_2}{\lambda_2}\le x\le 1\end{cases} \tag{10}$$

The corresponding boundary conditions are:

$$\left.\begin{aligned}
&w\ne 0,\theta=0,\phi=0,\text{ at } y=0\\
&w=0,\theta=1,\phi=1,\text{ at } y=h_\alpha
\end{aligned}\right\} \tag{11}$$

2.6. Perturbation of the System

We shall consider the oscillatory perturbation terms in order to reduce equations (7)-(11), following Bunonyo *et al*. [10], since the flow is caused by the pumping action of the heart. Hence the flow profiles are presented as follows:

$$\left.\begin{aligned}
&w=w_0e^{\omega t}\\
&\theta=\theta_0e^{\omega t}\\
&\phi=\phi_0e^{\omega t}\\
&\frac{\partial P}{\partial x}=P_0e^{\omega t}
\end{aligned}\right\} \tag{12}$$

Substituting equation (12) into equations (7)-(9), we have:

$$\frac{d^2w_0}{dy^2}-\beta_1^2w_0=P_0-Gr\theta_0-Gc\phi_0 \tag{13}$$

$$\frac{d^2\theta_0}{dy^2}+\beta_2^2\theta_0=-\phi_0Rd_2 \tag{14}$$

$$\frac{d^2\phi_0}{dy^2}-\beta_3^2\phi_0=0 \tag{15}$$

where

$\beta_1^2=\left(M^2+\omega+\frac{1}{k}\right),\beta_2^2=Pr\left(Rd_1-\omega\right)$, and $\beta_3^2=\left(Rd_3+\omega\right)Sc$

The boundary conditions at the first atherosclerotic region are:

$$\left.\begin{array}{ll} w_0 = w_a \neq 0, \theta_0 = 0, \phi_0 = 0, & \text{at } y = 0 \\ w_0 = 0, \theta_0 = e^{-\omega t} = \theta_a, \phi_0 = e^{-\omega t} = \phi_a, & \text{at } y = h_\alpha \end{array}\right\} \quad (16)$$

Solving equation (15), we have:

$$\phi_0 = c_1 sinh\beta_3 y + c_2 cosh\beta_3 y \quad (17)$$

Solving equation (16) using the cell free boundary conditions in equation (15), we have:

$$\phi_0 = c_1 sinh\beta_3 y \quad (18)$$

where $c_1 = \dfrac{e^{-\omega t}}{sinh\beta_3 h_\alpha}$

Simplifying equation (3), (16) using the normal boundary conditions, we have:

$$\phi_0(y) = \left(\frac{e^{-\omega t}}{sinh\beta_3 h_\alpha}\right) sinh\beta_3 y \quad (19)$$

Substituting equation (18) into equation (12), we have:

$$\phi(y,t) = \left(\frac{sinh\beta_3 y}{sinh\beta_3 h_\alpha}\right) \quad (20)$$

Substituting equation (18) into equation (14), we have:

$$\frac{d^2\theta_0}{dy^2} + \beta_2^2\theta_0 = -\left(\frac{Rd_2 e^{-\omega t}}{sinh\beta_3 h_\alpha}\right) sinh\beta_3 y \quad (21)$$

Simplifying equation (20), we have:

$$\frac{d^2\theta_0}{dy^2} + \beta_2^2\theta_0 = \beta_4 sinh\beta_3 y \quad (22)$$

where $\beta_4 = -\left(\dfrac{Rd_2 e^{-\omega t}}{sinh\beta_3 h_\alpha}\right)$

The particular part of equation (21) is:

$$\theta_{0p} = A\sinh\beta_3 y + B\cosh\beta_3 y \quad (23)$$

Differentiating equation (22) according to the order of equation (21), we have:

$$\frac{d^2\theta_{0p}}{dy^2} = A\beta_3^2 \sinh\beta_3 y + B\beta_3^2 \cosh\beta_3 y \quad (24)$$

Simplifying equations (21) and (23), we have:

$$A = \frac{\beta_4}{\left(\beta_3^2 + \beta_2^2\right)}, B = 0 \quad (25)$$

Substituting equation (24) into equation (22), we have:

$$\theta_{0p} = \frac{\beta_4}{\left(\beta_3^2 + \beta_2^2\right)} \sinh\beta_3 y \quad (26)$$

The general solution of equation (21), we have:

$$\theta_0 = c_3 sin\beta_2 y + c_4 cos\beta_2 y + \frac{\beta_4}{\left(\beta_3^2 + \beta_2^2\right)} sinh\beta_3 y \quad (27)$$

Solving for the constant coefficients in equation (26) using equation (16), we have:

$$\theta_0 = c_3 sin\beta_2 y + \frac{\beta_4}{\left(\beta_3^2 + \beta_2^2\right)} sinh\beta_3 y \quad (28)$$

Simplifying equation (27), we have:

$$c_3 = \frac{e^{-\omega t}}{sin\beta_2 h} - \frac{\beta_4 sinh\beta_3 h}{\left(\beta_3^2 + \beta_2^2\right) sin\beta_2 h} \quad (29)$$

Substituting equation (28) into equation (27), we have:

$$\theta_0 = \left(\frac{e^{-\omega t}}{sin\beta_2 h} - \frac{\beta_4 sinh\beta_3 h}{\left(\beta_3^2 + \beta_2^2\right) sin\beta_2 h}\right) sin\beta_2 y + \frac{\beta_4}{\left(\beta_3^2 + \beta_2^2\right)} sinh\beta_3 y \quad (30)$$

$$\theta_0 = c_3 sin\beta_2 y + \frac{\beta_4}{\left(\beta_3^2 + \beta_2^2\right)} sinh\beta_3 y \quad (31)$$

Substituting equations (30)-(18), we have:

$$\frac{d^2w_0}{dy^2}-\beta_1^2w_0=P_0-\left(c_3Grsin\beta_2y+\frac{\beta_4Gr}{\left(\beta_3^2+\beta_2^2\right)}sinh\beta_3y\right)-\left(\frac{Gce^{-\omega t}}{sinh\beta_3h_\alpha}\right)sinh\beta_3y \tag{32}$$

$$\frac{d^2w_0}{dy^2}-\beta_1^2w_0=P_0-\left(c_3Grsin\beta_2y\right)-\left(\frac{\beta_4Gr}{\left(\beta_3^2+\beta_2^2\right)}+\frac{Gce^{-\omega t}}{sinh\beta_3h_\alpha}\right)sinh\beta_3y \tag{33}$$

$$\frac{d^2w_0}{dy^2}-\beta_1^2w_0=P_0-c_3Grsin\beta_2y-\left(\frac{\beta_4Gr}{\left(\beta_3^2+\beta_2^2\right)}+c_1Gc\right)sinh\beta_3y \tag{34}$$

If $c_5=\left(\frac{\beta_4Gr}{\left(\beta_3^2+\beta_2^2\right)}+c_1Gc\right)$, then equation (34) becomes:

$$\frac{d^2w_0}{dy^2}-\beta_1^2w_0=P_0-c_3Grsin\beta_2y-c_5sinh\beta_3y \tag{35}$$

The homogenous solution of equation (35) is:

$$w_{0h}=c_{51}sinh\beta_1y+c_6cosh\beta_1y \tag{36}$$

The particular part in equation (35) is:

$$w_{0p}=c_7+c_8sin\beta_2y+c_9sinh\beta_3y \tag{37}$$

Differentiating equation (37), we have:

$$\frac{d^2w_{0p}}{dy^2}=c_9\beta_2^2sinh\beta_3y-c_8\beta_2^2sin\beta_2y \tag{38}$$

The general solution of equation (35) is the sum of equation (35) and (36), which is:

$$w_0=c_{51}sinh\beta_1y+c_6cosh\beta_1y+c_7+c_8sin\beta_2y+c_9sinh\beta_3y \tag{39}$$

Solving for the constant coefficients in equation (39) using equation (16), we have:

$$\left.\begin{aligned}c_6&=\left(w_a-c_7\right),c_7=-\frac{P_0}{\beta_1^2},c_8=\frac{Grc_3}{\left(\beta_2^2+\beta_1^2\right)},c_9=\frac{c_5}{\left(\beta_1^2-\beta_2^2\right)}\\c_{51}&=c_7\frac{\left(cosh\beta_1h_a-1\right)}{sinh\beta_1h_a}-w_a\frac{cosh\beta_1h_a}{sinh\beta_1h_a}-c_8\frac{sin\beta_2h_a}{sinh\beta_1h_a}-c_9\frac{sinh\beta_3h_a}{sinh\beta_1h_a}\end{aligned}\right\} \tag{40}$$

Simplified solution of equation (39) is:

$$w_0=c_{51}sinh\beta_1y+w_acosh\beta_1y+c_7\left(1-cosh\beta_1y\right)+c_8sin\beta_2y+c_9sinh\beta_3y \tag{41}$$

Substituting equation (41) into equation (12), we have:

$$w=\left(c_{51}sinh\beta_1y+w_acosh\beta_1y+c_7\left(1-cosh\beta_1y\right)+c_8sin\beta_2y+c_9sinh\beta_3y\right)e^{i\omega t} \tag{42}$$

3. Results

The analytical solution will be numerically simulated in this part, and the results will be shown graphically. The simulation's data came from Bunonyo *et al*. [10], Bunonyo and Ndu [11], Butter *et al*. [13], and the outcomes are shown as follows:

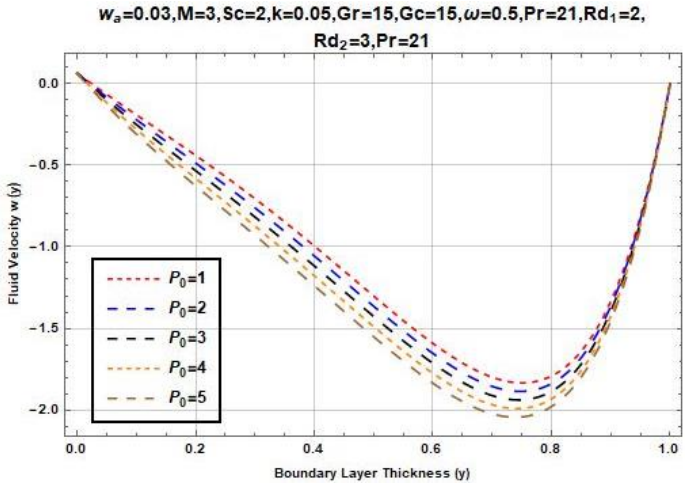

Figure 1. *The effect of Pressure changes on Fluid Velocity Profile.*

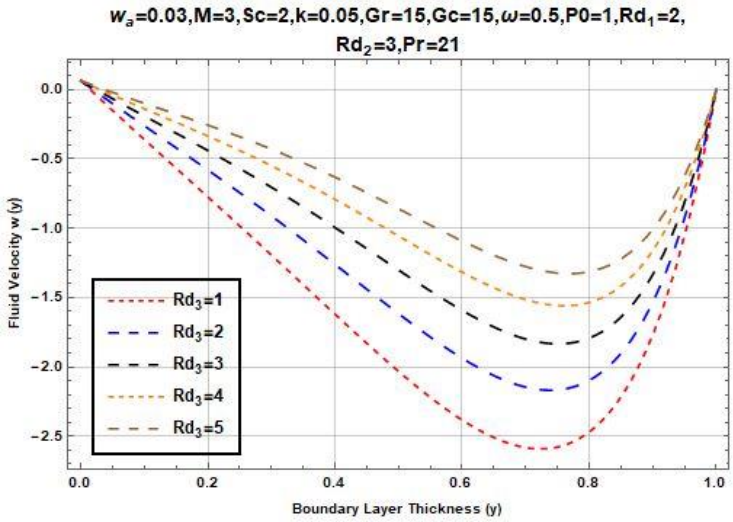

Figure 2. *The effect of Chemical reaction on Fluid Velocity Profile.*

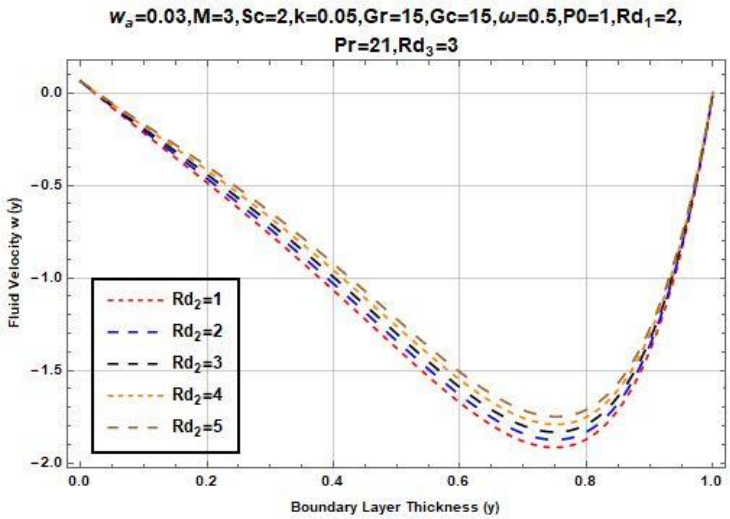

Figure 3. *The effect of Mass source on Fluid Velocity Profile.*

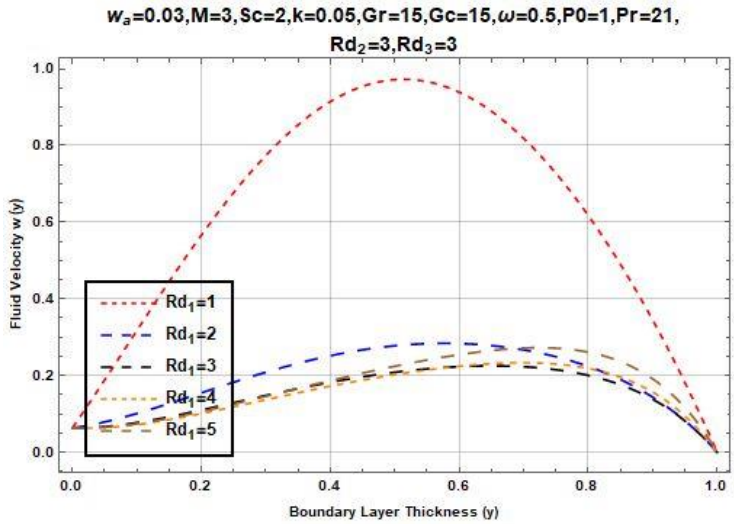

Figure 4. *The effect of radiation parameter on Fluid Velocity Profile.*

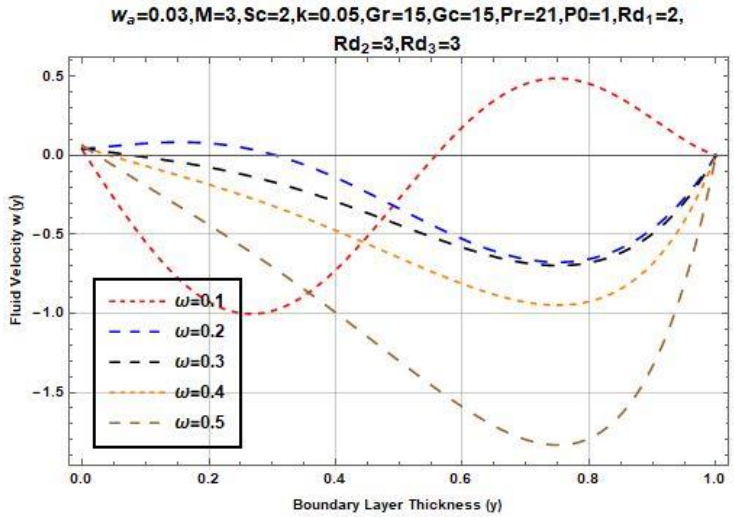

Figure 5. *The effect of oscillatory frequency on Fluid Velocity Profile.*

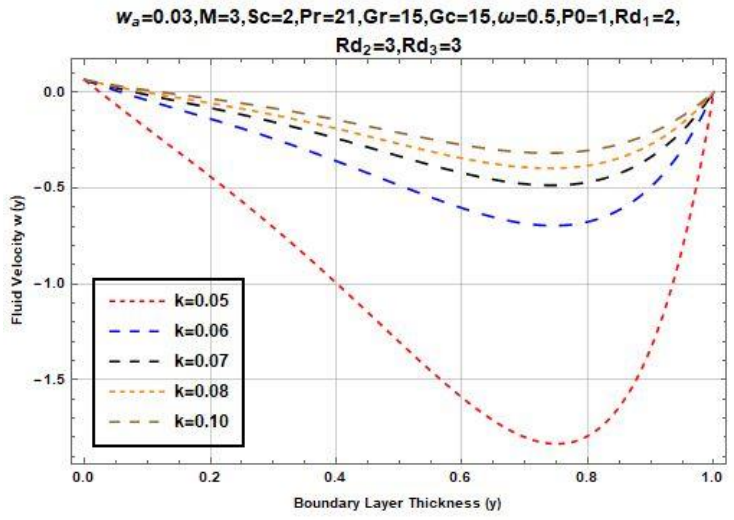

Figure 6. *The effect of Porosity on Fluid Velocity Profile.*

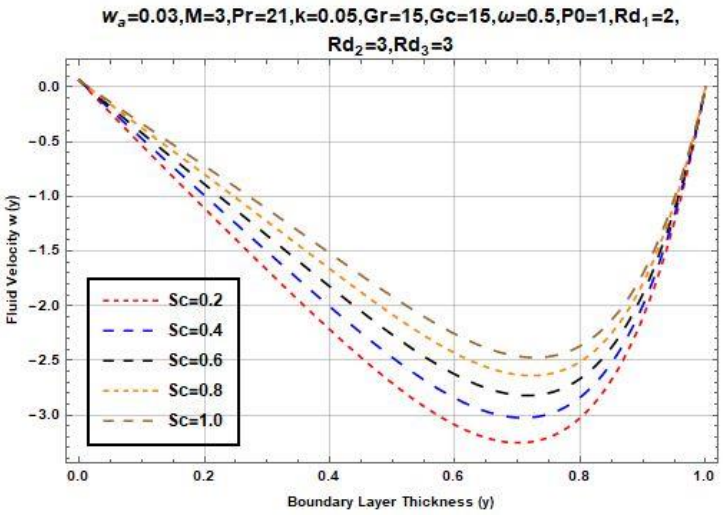

Figure 7. *The effect of Schmidt number on Fluid Velocity Profile.*

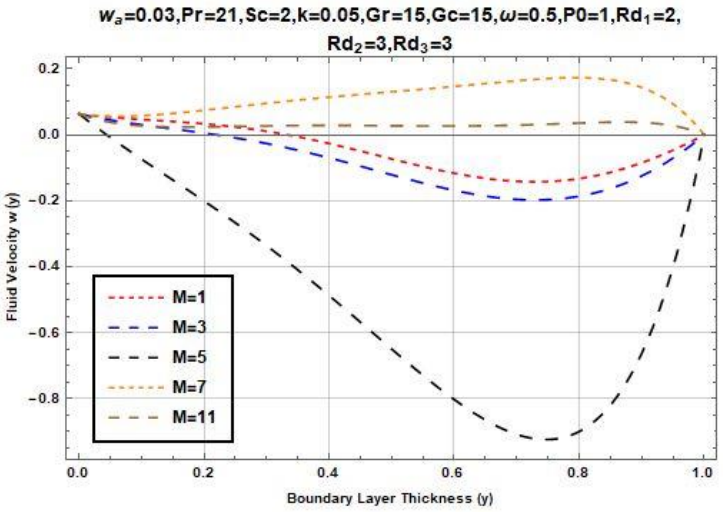

Figure 8. *The effect of Hartman number on Fluid Velocity Profile.*

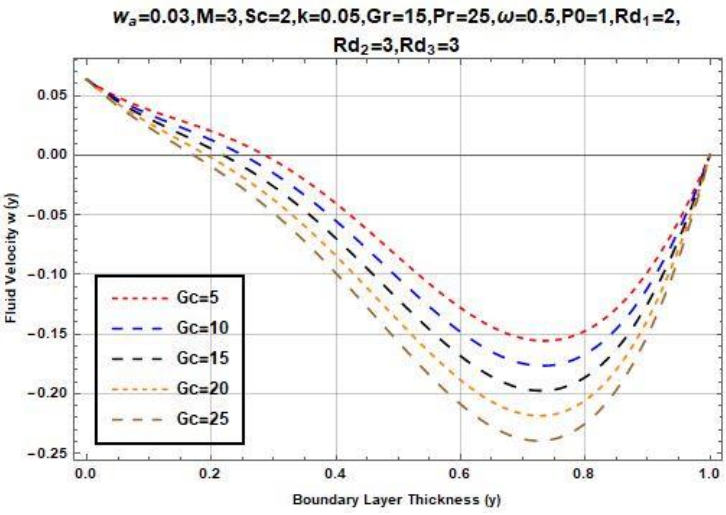

Figure 9. *The effect of solutal Grashof number on Fluid Velocity Profile.*

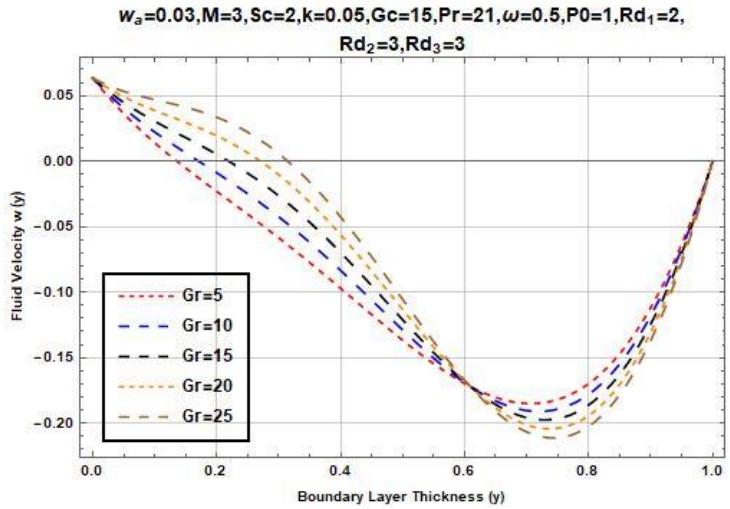

Figure 10. *The effect of Grashof number on Fluid Velocity Profile.*

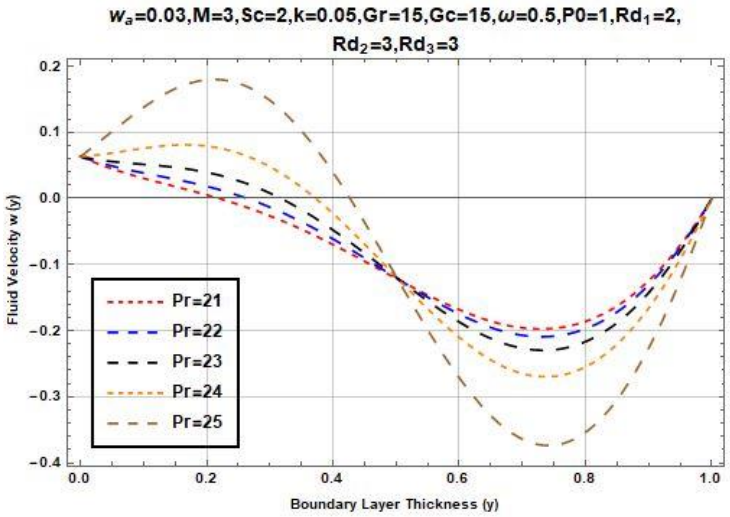

Figure 11. *The effect of Prandtl number on Fluid Velocity Profile.*

4. Discussion

This research is a novelty in the aspect of investigating the role sickle cell diseases play in the formation of plaques and atherosclerosis due to mass concentration of sickle cells. In furtherance to that, we shall discuss the flow profiles as follows: Figure 1 depicts the effect of pressure change on fluid velocity. The result showed that an increase in pressure gradient leads to a reduction in fluid velocity within the boundary layer. Higher pressure opposes fluid motion, increasing resistance to flow. The velocity boundary layer becomes thinner as pressure increases. The physical implication is that a strong adverse pressure gradient suppresses fluid motion, a common phenomenon in porous and biofluid systems. This trend is consistent with classical boundary-layer theory and agrees with Makinde [22], who reported similar retardation in porous channel flows. The effect of chemical reaction on fluid velocity was investigated, and the result shown in Figure 2 is that increasing the chemical reaction parameter causes a decrease in velocity, because the chemical reactions consume species and energy, thereby reducing momentum transport. In essence, stronger reactions enhance molecular interactions that dampen the flow. This occurs because reactive processes deplete species and energy, thereby weakening momentum transport. Comparable findings were reported by Chamkha [23] and Afify [24], where chemical reactions acted as a decelerating force in MHD flows.

In this Figure 3, we investigated the effect of mass source on fluid velocity, where it can be seen that increasing the magnitude of mass source strength enhances fluid velocity. It means that the additional mass injected into the system contributes to momentum gain. Its relevance in biological fluids such as blood is that it helps in cell proliferation or drug dif-

fusion which agrees with Makinde and Aziz [25], who observed that mass injection accelerates boundary-layer development. Figure 4 depicts that higher radiation levels result in increased velocity profiles, and it talks about the effect of radiation on velocity profiles. The thermal radiation adds energy to the system, reducing fluid viscosity effects because radiation heat transfer promotes fluid acceleration and this observation is consistent with Raptis et al. [26], where radiative heat transfer enhanced fluid motion. The effect of oscillatory frequency on fluid velocity was investigated, and it was noted that increasing oscillatory frequency significantly reduces velocity magnitude based on the result shown in Figure 5. The flow becomes more resistant as oscillations intensify, and rapid oscillations enhance viscous dissipation and suppress momentum diffusion, this is so because the oscillatory frequency reduces velocity due to increased viscous dissipation and flow resistance induced by rapid oscillations. This behavior aligns with Soundalgekar [27], who showed that oscillatory motion dampens flow velocity. Figure 6 investigated the effect of porosity on the fluid velocity, and it was found that higher porosity values lead to higher velocity profiles. Reduced resistance from the porous medium allows easier fluid passage. The implication is that highly porous media support better flow circulation and this is in agreement with Nield and Bejan [28], who demonstrated that increased porosity facilitates fluid transport. Figure 7 showed the effect of the Schmidt number on fluid velocity was investigated, and the result showed that increasing the Schmidt number results in lower velocity profiles. It's of the view that a high Schmidt number implies low mass diffusivity, weakening momentum coupling. We observed that the momentum transfer is reduced when mass diffusion is weak. This agrees with Gebhart et al. [29]. The effect of the Hartmann number on fluid velocity was investigated; it showed in Figure 8 that increasing the Hartmann number causes a significant reduction in velocity. Magnetic fields introduce Lorentz forces that oppose fluid motion. The magnetic damping strongly suppresses electrically conducting flows. This is a classical magnetohydrodynamic effect, consistent with Hartmann [30] and Shercliff [31]. Figure 9 illustrates the effect of the solutal Grashof number on fluid velocity, and it can be seen that velocity increases with increasing solutal Grashof number. Concentration buoyancy enhances fluid motion. In conclusion, species concentration gradients significantly drive convection. The effect of the Grashof number on fluid velocity was investigated, and the result is presented graphically as Figure 10. The result showed that higher Grashof numbers produce higher velocity profiles. Stronger thermal buoyancy dominates viscous forces. In general, both solutal and thermal Grashof numbers (Figures 9 and 10) significantly enhance velocity due to buoyancy forces. These results agree with Ostrach [32] and Bejan [33], confirming that natural convection strengthens fluid motion. The effect of the Prandtl number on the fluid velocity was investigated, and results are presented in Figure 11, and the result shows that the increasing Prandtl number reduces velocity. Higher Prandtl number fluids have lower thermal diffusivity. The implication is that momentum diffusion dominates over thermal diffusion at high Prandtl numbers. This observation agrees with Incropera and DeWitt [34].

5. Conclusion

This work used mathematical modeling and computer analysis to examine the combined effects of temperature gradients, high sickle cell concentration, and an applied magnetic field on blood circulation through a porous atherosclerotic channel. The findings show that elevated sickle cell concentration considerably reduces blood flow because of increased effective viscosity and changed rheological characteristics, which result in lower velocity profiles. Convective transport is improved by the existence of a temperature gradient, which raises the rates of mass and thermal energy transfer inside the channel. In the meantime, flow velocity is dampened and temperature and concentration distributions are altered by the resistive (Lorentz) force exerted by the applied magnetic field. Additionally, the research demonstrates that these effects are mediated by the atherosclerotic channel's porosity, with larger porosity facilitating simpler blood transit. In summary, the study offers quantitative insights into the intricate relationships between hemodynamic, thermal, and magnetic effects in pathological blood flow conditions, potentially providing direction for therapeutic interventions in sickle cell disease and atherosclerosis patients, such as targeted magnetic or thermal treatments.

These findings are in strong agreement with classical and modern studies, including those of Hartmann [30], Ostrach [32], Makinde [22], and more recent investigations, Shahbaz and Ahmad, 2024 [35], all of which confirm magnetic damping and buoyancy-driven acceleration in MHD flows. These findings provide valuable insight for the design and optimization of biomedical and engineering systems involving MHD flow in porous structures.

Abbreviations

y^*	Dimensional Vertical Distance
C^*	Dimensional Cell Mass Concentration
T^*	Dimensional Temperature
C_∞	Far field Cell Mass Concentration
T_∞	Far field Temperature
Q_0	Heat Source Due to Temperature
Q_1	Cell Mass Concentration Source
ρ_b	Blood Density
c_{bp}	Blood Specific Heat Capacity
k_{bT}	Blood Thermal Conductivity
D_m	Mass Diffusivity

k_0	Chemical Reaction
k_T	Lipid Concentration Treatment
t^*	Dimensional Time
Rd_1	Heat Source Term
Rd_2	Cell Mass Concentration Source Term
Rd_3	Chemical Reaction Term
ϕ	Dimensionless Cell Mass Concentration
θ	Dimensionless Temperature
Pr	Prandtl Number of Blood
Sc	Schmidt Number
M	Magnetic Field Parameter
k	Porosity
Gr	Grashof Number
Gc	Solutal Grashof Number
ω	Oscillatory Frequency Parameter

Acknowledgments

We would like to take this opportunity to thank the Tertiary Education Trust Fund (TETFUND) for providing the funds required to make this study a success.

Author Contributions

Kubugha Wilcox Bunonyo: Conceptualization, Formal analysis, Methodology, Resources, Software, Project administration, Validation, Visualization, Supervision, Funding acquisition, Writing – original draft, Writing – review & editing

Anasuodei Bemoifie Moko: Data curation, Project administration, Validation, Visualization, Supervision, Resources, Writing – review & editing

Tamuno Boma Odinga-Israel: Data curation, Project administration, Supervision, Investigation, Resources, Writing – review & editing

Conflicts of Interest

There is no conflict of interest of any kind.

References

[1] Abdelsalam, S. I., & Vafai, K. (2017). Particulate suspension effect on peristaltically induced unsteady pulsatile flow in a narrow artery: blood flow model. *Mathematical biosciences*, 283, 91-105. https://doi.org/10.1016/j.mbs.2016.11.012

[2] Abdullah, I., Amin, N., & Hayat, T. (2011). Magnetohydrodynamic effects on blood flow through an irregular stenosis. Int J Numer Methods Fluids, 67(11), 1624-1636. https://doi.org/10.1002/fld.2436

[3] Acosta, S., Puelz, C., Rivi ère, B., Penny, D. J., & Rusin, C. G. (2015). Numerical method of characteristics for one-dimensional blood flow. *Journal of computational physics*, 294, 96-109. https://doi.org/10.1016/j.jcp.2015.03.045

[4] Ahmed, A., & Nadeem, S. (2016). The study of (Cu, TiO2, Al2O3) nanoparticles as antimicrobials of blood flow through diseased arteries. *Journal of Molecular Liquids*, 216, 615-623. https://doi.org/10.1016/j.molliq.2016.01.059

[5] Alasakani, K., Tantravahi, S. L. R., & Kumar, P. (2020). An Approach to Identify Significant Parameters in Blood Flow through Human Arteries. *Science & Technology Asia*, 95-105. https://doi.org/10.14456/scitechasia.2020.10

[6] Amos, E., &Ogulu, A. (2003). Magnetic effect on pulsatile flow in a constricted axis-symmetric tube. *Indian Journal of Pure & Applied Mathematics*, 34(9), 1315-1326.

[7] Bunonyo, K. W., & Amos, E. (2020). Impact of treatment parameter on blood flow in an atherosclerotic artery. *American Journal of Theoretical and Applied Statistics*, *9*(3), 74. https://doi.org/10.11648/j.ajtas.20200903.17

[8] Baroncini, L. A. V., de Castro Sylvestre, L., &Pecoits Filho, R. (2015). Carotid intima-media thickness and carotid plaque represent different adaptive responses to traditional cardiovascular risk factors. *International journal of cardiology. Heart &vasculatur*8(9), 48-51. https://doi.org/10.1016/j.ijcha.2015.08.003

[9] Balkaran, B., Char, G., Morris, J. S., Thomas, P. W., Serjeant, B. E., & Serjeant, G. R. (1992). Stroke in a cohort of patients with homozygous sickle cell disease. *The Journal of pediatrics*, *120*(3), 360-366. https://doi.org/10.1016/S0022-3476(05)80897-2

[10] Bunonyo, K. W, Moko, A. B, & Tamuno Boma Odinga (2026) Computational Approach in Mathematical Modeling of Cell Mass Concentration Effect on Heat Transfer Through a Blood Channel. Journal of Mathematical & Computer Applications. SRC/JMCA-281. https://doi.org/doi.org/10.47363/JMCA/2026(5)236

[11] Bunonyo, K. W., &Ndu, R. I. (2024). Mathematical Modelling and Numerical Simulation of Haematocrit and Pressure Effects on Blood Flow through Blood Vessel. *International Research Journal of Pure and Applied Physics*, *11*(1), 132-143. https://doi.org/10.37745/irjpap.13vol11n1132143

[12] Bunonyo, K. W., & Dagana, J. T. (2024). Mathematical Modelling of the Impact of Mass Concentration on Viscoelastic Fluid Flow through a Non-Porous Channel. *Asian Journal of Pure and Applied Mathematics*, *6*(1), 253-270. Accessed from: https://jofmath.com/index.php/AJPAM/article/view/171

[13] Butter, J. K., Bunonyo, K. W., & Eli, I. C. (2024). Mathematical Modelling of the Thermosolutal Effect on Blood Flow through a Micro-Channel in the Presence of a Magnetic Field. *British Journal of Multidisciplinary and Advanced Studies*, *5*(4), 14-32. https://doi.org/10.37745/bjmas.2022.04161

[14] Bunonyo, K. W., Ebiwareme, L., &Iworiso, P. B. (2024). Mathematical modeling of time-dependent concentration of alcohol in the human bloodstream using the eigenvalue method. *TWIST*, *19*(1), 58-64. https://doi.org/10.5281/zenodo.10049652

[15] Bunonyo, K. W., Ebiwareme, L., &Igodo, A. (2026). Mathematical Examination of MHD Slip Oscillatory Blood Flow Through an Artery in a Magnetic Field. *Journal of Physical Mathematics & its Applications. SRC/JPMA-174. (4), 145*, 2-6. https://doi.org/10.47363/JPMA/2026

[16] Bunonyo, K. W., Peter, B., &Okrinya, A. B. (2026). Application of Piezoelectric Properties in Understanding Voltage Generation, Displacement, and Acceleration via Packed Sickle Cell. *Asian Journal of Pure and Applied Mathematics*, *8*(1), 119-136. https://doi.org/10.56557/ajpam/2026/v8i1256

[17] Daniel, M., Szymanik-Grzelak, H., Sierdziński, J., Podsiadły, E., Kowalewska-Młot, M., &Pańczyk-Tomaszewska, M. (2023). Epidemiology and risk factors of UTIs in children—A single-center observation. *Journal of personalized medicine*, *13*(1), 138. https://doi.org/10.3390/jpm13010138

[18] Tziakas, D. N., Chalikias, G., Pavlaki, M., Kareli, D., Gogiraju, R., Hubert, A.,...& Schäfer, K. (2019). Lysed erythrocyte membranes promote vascular calcification: possible role of erythrocyte-derived nitric oxide. *Circulation*, *139*(17), 2032-2048. https://doi.org/10.1161/CIRCULATIONAHA.118.037166

[19] Serjeant, G. R. (2005). Mortality from sickle cell disease in Africa. *Bmj*, *330*(7489), 432-433. https://doi.org/10.1136/bmj.330.7489.432

[20] Makani, J., Ofori-Acquah, S. F., Nnodu, O., Wonkam, A., & Ohene-Frempong, K. (2013). Sickle cell disease: new opportunities and challenges in Africa. *The scientific world journal*, *2013*(1), 193252. https://doi.org/10.1155/2013/193252

[21] Rees, D. C., Williams, T. N., & Gladwin, M. T. (2010). Sickle-cell disease. *The Lancet*, *376*(9757), 2018-2031. https://doi.org/10.1016/S0140-6736(10)61029-X

[22] Makinde, O. D. (2008). Effects of viscous dissipation and radiation on MHD flow. *Applied Mathematics and Computation*, 201, 322-329.

[23] Chamkha, A. J. (2003). MHD flow with heat and mass transfer and chemical reaction. *International Journal of Engineering Science*, 41, 647-662.

[24] Afify, A. A. (2004). Effects of heat and mass transfer on MHD flow. *Heat and Mass Transfer*, 40, 495-500. https://doi.org/10.1007/s00231-003-0486

[25] Makinde, O. D., & Aziz, A. (2011). Boundary layer flow with mass transfer. *International Journal of Thermal Sciences*, 50, 1326-1332. https://doi.org/10.1016/j.ijthermalsci.2011.02.019

[26] Raptis, A., Perdikis, C., & Takhar, H. (2004). Effect of thermal radiation on flow. *Applied Mathematics and Mechanics*, 25, 113-121.

[27] Soundalgekar, V. M. (1979). Oscillatory flow past a plate. *Journal of Applied Mechanics*.

[28] Nield, D. A., & Bejan, A. (2013). *Convection in Porous Media* (4th ed.). Springer. https://doi.org/10.1007/978-1-4614-5541-7

[29] Gebhart, B., Jaluria, Y., Mahajan, R. L., &Sammakia, B. (1988). *Buoyancy-Induced Flows and Transport*. Hemisphere.

[30] Hartmann, J. (1937). Hg-dynamics I. *Kgl. Danske Videnskabernes Selskab*.

[31] Shercliff, J. A. (1965). *A Textbook of Magnetohydrodynamics*. Pergamon.

[32] Ostrach, S. (1953). Natural convection in fluids. *NACA Report*.

[33] Bejan, A. (2013). *Convection Heat Transfer* (4th ed.). Wiley. https://doi.org/10.1002/9781118671627

[34] Shahbaz, H. M., & Ahmad, I. (2024). Numerical treatment for Darcy-Forchheimer flow under MHD effects. *Scientific Reports*, 14, 31214. https://doi.org/10.1038/s41598-024-82569-3

[35] Shahbaz, H. M., & Ahmad, I. (2024). Numerical treatment for Darcy-Forchheimer flow under MHD effects. *Scientific Reports*, 14, 31214. https://doi.org/10.1038/s41598-024-82569-3